Co-option of neurotransmitter signaling for inter-organismal communication in *C. elegans*

Christopher D. Chute[1], Veronica L. Coyle[1+,], Ying K. Zhang[2], Diego Rayes[3], Hee June Choi[4] Mark Alkema[3], Frank C. Schroeder[2], Jagan Srinivasan[1*]

[1]Biology and Biotechnology Department, Worcester Polytechnic Institute, Worcester, Massachusetts 01605

[2]Boyce Thompson Institute and Department of Chemistry and Chemical Biology, Cornell University, Ithaca, New York 14853

[3] Neurobiology Department, University of Massachusetts Medical School, Worcester, Massachusetts 01605

[4] Biomedical Engineering Department, Worcester Polytechnic Institute, Worcester, Massachusetts 01605

[+] Present address: AbbVie, Worcester, Massachusetts, 01605

[*]To whom correspondence should be addressed. Tel.: 508-831-6564; E-mail: jsrinivasan@wpi.edu

Abstract

Biogenic amine neurotransmitters play a central role in metazoan nervous systems, and both their chemical structures and cognate receptors are evolutionarily highly conserved. In the nematode *C. elegans*, four classical neurotransmitters - serotonin, dopamine, octopamine, and tyramine - have been detected and appear to serve signaling functions related to those in insects or vertebrates (1). Interestingly, one of the small molecule pheromones released by *C. elegans* incorporates the monoamine octopamine. Octopamine succinylated ascaroside #9 (osas#9) is biochemically derived by connecting the neurotransmitter octopamine to an ascaroside – a universal building block of pheromones in *C. elegans* (2, 3). Neuronal ablation, cell-specific genetic rescue, and calcium imaging show that *tyra-2,* a gene coding for a G protein-coupled receptor (GPCR), expression in the nociceptive neuron ASH is both necessary and sufficient to induce avoidance of osas#9. In contrast, expression of *tyra-2* in AWA, a neuron pair primarily involved in attraction, reverses the behavioral response to osas#9. These results show that TYRA-2 serves as a receptor for the neurotransmitter-derived osas#9, and thus may function in both internal signaling and sensation of external signals. The TYRA-2/osas#9 signaling system thus provides an example for the evolution of an inter-organismal communication channel via co-option of a small-molecule signal and its cognate receptor.

Author Summary

Inter-organismal chemical communication relays information from one organism to another, and elicits specific behaviors in the receiving organism via downstream intra-organismal signaling pathways. Given the ancient origin of chemical communication, it seems plausible that evolution would favor re-use parts of the communication machinery. Previous work had identified the neurotransmitter-derived pheromone osas#9 which elicits avoidance behavior in conspecific *C. elegans*. Based on the assumption that additional components of neurotransmitter signaling may have been co-opted for perception of osas#9, we conducted a reverse genetic screen of neurotransmitter receptors and identified *tyra-2*, a tyramine/octopamine receptor as required for the osas#9 avoidance response. These results suggest that this signaling pathway has re-purposed a neurotransmitter by "packaging" it into a pheromone molecule and retained the receptor of this neurotransmitter to sense this signal. Our findings reveal dual use of neurotransmitter communication machinery linking inter- and intra-organismal signaling.

Introduction

The proper coordination and execution of social behaviors is crucial for organismal survival. Social behaviors require effective inter-organismal communication strategies, as well as dedicated intra-organismal signaling pathways downstream of signal perception. Inter-organismal communication occurs in several forms across the animal kingdom, both within and between species: prairie dogs use audio alarm calls to signal danger to conspecifics (4), birds display ornate visual cues and dances to attract mates (5), and honeybees dance to signal food location (6). Less apparent, though ancient and ubiquitous across all kingdoms of life, is chemical communication, which underlies social responses driven by chemosensation (7-10). Chemical communication requires both intra- and inter- organismal signaling: first, a chemical cue is released into the environment by one organism that is then detected by specific receptors in another organism. Upon perception, intra-organismal signaling pathways, e.g. neurotransmitter signaling, are activated that ultimately coordinate a social response.

A major class of neurotransmitters are the biogenic monoamines dopamine, serotonin, or adrenaline, which along with chemically related compounds tyramine and octopamine can be found throughout life, from plants to animals (11). Intra-organismal neurotransmitter communication involves often highly regulated compound biosynthesis, translocation, either by way of diffusion or through active transport, and finally perception by dedicated chemoreceptors. Many neurotransmitters are perceived via GPCRs, in fact, there appears to be a close relationship between GPCR diversification and neurotransmitter synthesis in shaping neuronal systems (12). Notably, the most common neurotransmitters share similar behavioral functions across phyla, for example, serotonin is commonly involved in regulating food responses (13, 14). Given the role of GPCR-based neurotransmitter signaling in coordinating responses across phyla, we hypothesized that similar monoamine signaling systems may underlie chemical communication between organisms.

Our investigations utilize the nematode *Caenorhabditis elegans* as it affords many advantages for studying social chemical communication and neuronal signaling, due to the animal's tractability, well-characterized nervous system, and social behavioral responses to pheromones (15, 16). The nematode secretes a class of small-molecules known as ascarosides, which serve diverse functions in inter-organismal chemical signaling (17-19). As a core feature, these molecules include an ascarylose sugar attached to a fatty acid-derived side chain that can be

optionally decorated with building blocks from other primary metabolic pathways (3). Ascaroside production, and thus secretory profile as chemical messengers, is strongly dependent on the animal's sex, life stage, environment, and physiological state (2, 20-22). Depending on their specific chemical structures and concentration, the effects of ascaroside signaling vary from social (e.g. attraction to icas#3) to developmental (e.g. induction of dauer by ascr#8) (Fig. 1A) (22-25). Furthermore, different combinations of these ascarosides can act synergistically to elicit a stronger behavioral response than one ascaroside alone, such as male attraction to ascr#2, ascr#3, and ascr#4 (18). Several G-protein coupled receptors (GPCRs) have been identified as chemoreceptors of ascaroside pheromones, such as SRX-43 in ASI in dwelling behavior and DAF-37 in ASK in hermaphrodite repulsion (26-30).

Notably, one particular ascaroside that mediates social interactions is derived from octopamine, a common neurotransmitter found to endogenously control behavior (31). As such, we investigated the role of this compound as a link between inter- and intra-organismal signaling. Here we show that TYRA-2, an endogenous trace amine receptor, also functions as a chemoreceptor for osas#9, demonstrating co-option of intra-organismal neurotransmitter synthesis and pathways involved in inter-organismal communication.

Results

Aversive responses to osas#9 require the GPCR TYRA-2

The ascaroside osas#9 (Fig. 1A) was found to be produced specifically by developmentally arrested larval stage one (L1 stage) *C. elegans* (2). Using a behavioral drop test assay, we confirmed that osas#9 elicits avoidance behavior in starved *C. elegans* of both sexes and all developmental stages (Fig. 1B,C) (2). We found that osas#9 is active over a very broad range of concentrations (fM - μM) (Fig. 1D). Ascarosides such as the male attractant ascr#3 and aggregation ascaroside icas#3 show activity profiles that are similarly broad as that of osas#9, whereas others, such as the mating cue ascr#8, are active only within more narrow concentration ranges (23, 32, 33). As osas#9 avoidance is dependent upon starvation, we propose that osas#9 serves as a dispersal signal when a food patch is depleted (Fig. 1E,F).

The chemical structure of osas#9 is unusual in that it includes the neurotransmitter octopamine as a building block. Because octopamine and the biosynthetically related neurotransmitter tyramine play important roles in orchestrating aversive responses, we

investigated tyramine (*tyra-2, tyra-3, ser-2, and ser-3*) and octopamine (*ser-3, ser-6, and octr-1*) receptors for potential involvement in the osas#9 response (Fig. 2A) (34-38). We found that avoidance responses to osas#9 are largely abolished in *tyra-2 lof* mutants and RNAi knockdown (Fig. 2A, S1A), which encodes for a GPCR capable of binding tyramine *in vitro* (34). Next, we designed a *tyra-2* rescue construct consisting of the entire genomic locus, including 2kb upstream, fused to GFP (*tyra-2p::tyra-2::*GFP). Indeed, *tyra-2* expression under its native promoter reconstituted wild-type osas#9 aversion in *tyra-2 lof* animals (Fig. 2B). Taken together, our data supports that osas#9 avoidance response requires the GPCR TYRA-2.

Since *tyra-2* has been shown previously to bind tyramine, we asked whether tyramine signaling is required for the osas-9 avoidance response and examined *tdc-1 lof* mutants, which lack the ability to synthesize tyramine and octopamine (31, 34). We found that the behavioral response to osas#9 was unaltered in animals lacking tyramine synthesis (Fig. 2C). These results indicate that tyramine signaling is not required for osas-9 avoidance and suggest that *tyra-2's* function in osas#9 avoidance may involve interaction with a ligand other than tyramine. To exclude the possibility that *tyra-2* is necessary for reversals in general, we subjected *tyra-2 lof* animals to three well-studied chemical deterrents SDS, $CuCl_2$, or glycerol. No defects were found in the animals' ability to respond aversively to these deterrents (Fig. S1B). This indicates that the *tyra-2* is specifically required for osas#9 avoidance and is not part of a generalized unisensory avoidance response circuit.

tyra-2 is required in ASH sensory neuron for response to osas#9

To determine the site of *tyra-2* action in osas#9 avoidance we imaged TYRA-2::GFP and observed TYRA-2 expression in four sensory neurons: ASH, ASE, ASG, and ASI (Fig. 2D). These results are in agreement with previous studies on *tyra-2* expression (34). Next, we laser-ablated individual amphid sensory neurons to determine if a *tyra-2* expressing sensory neuron is required for the response. This revealed that ASH is the primary neuronal sensory pair required for the osas#9 response, whereas ablation of other neurons did not have a significant effect on this phenotype when comparing to their solvent control or wildtype osas#9 response (Fig. 3A, S2A). Furthermore, we found that ASH-specific rescue of *osm-9* expression, which is required for nociceptive signal transduction, is sufficient to restore response to osas#9 in *osm-9* mutants (Fig. 3B), confirming that ASH is the primary neuronal pair for osas#9 sensation (Fig. 3B) (39-42).

As ASH expresses *tyra-2* and is required for the response, we asked whether ASH-specific rescue of *tyra-2* restores osas#9 avoidance in *tyra -2* mutants. Expression of *tyra-2* under the *nhr-79* promoter, which is expressed in the ASH and ADL neurons, fully restored the avoidance response to osas#9 (Fig. 3C,D) (43). To ensure that the expression of *tyra-2* in ADL neurons was not responsible for the rescued phenotype, ADL neurons were ablated in the transgenic rescue line, and animals were observed to still avoid osas#9 (Fig. 3D). Taken together, these results indicate that *tyra-2* expression in ASH neurons is required for the behavioral response to osas#9.

To test whether the apparent role of ASH and *tyra-2* in osas#9 sensation, we utilized a modified microfluidic olfactory imaging chip that enables detection of calcium transients in sensory neurons (Fig. 3E,F) (44, 45). We observed that, upon exposure to osas#9, wild-type animals expressing GCaMP3 in the ASH neuron exhibit robust increases in fluorescence (Fig. 3A,B and Supp. video 1). Animals lacking *tyra-2* displayed no changes in fluorescence upon osas#9 exposure (Fig. 3E,F). This implies that *tyra-2* is required in the ASH sensory neuron to sense osas#9. To determine the subcellular localization of TYRA-2, we imaged *tyra-2p::*TYRA-2*::*GFP reporter construct and revealed the presence of *tyra-2* in both the cilia and the soma of the ASH neurons (Fig. 4A). As TYRA-2 was observed to be present in the cilia, we hypothesized that testing its known ligand, tyramine, for avoidance in the drop assay would result in aversive behavior. Interestingly, we found that at higher concentrations than osas#9 tyramine elicited an aversive response, but only when *tyra-2* was expressed in ASH (Fig. S3). On the other hand, at high concentrations of octopamine, repulsion appeared independent from *tyra-2* (Fig. S3)

Previous studies have shown that chemoreceptor expression levels change upon food deprivation. For instance, starved *C. elegans* increase olfactory receptor *odr-10* expression and down-regulate *srh-234* (46, 47). This is seen in other taxa as well, e.g. mosquitos, where down-regulation of the olfactory receptor AgOr1 occurs after satiety (48). Measuring *tyra-2* expression levels in both starved and well-fed animals using RT-qPCR, we found that starved animals exhibit a nearly two-fold increase in *tyra-2* expression (Fig. 4B). Our observations suggest that *tyra-2* expression is regulated by the physiological status of the animals and coincides with the behavioral response being dependent upon starvation (Fig 1E). This data, in conjunction with the localization of TYRA-2 to the cilia, and the lack of necessity for endogenous tyramine in the response to osas#9 indicate that *tyra-2* may be directly involved as a chemoreceptor for osas#9.

tyra-2 expression in AWA suggests osas#9 chemoreceptor

To determine if TYRA-2 is sufficient for sensing the pheromone osas#9, we reprogrammed another sensory neuron to ectopically express *tyra-2*. Previous studies in *C. elegans* indicate that behavioral responses elicited by an odorant are specified by the olfactory neuron in which the receptor is activated in, rather than by the olfactory receptor itself (49). Since AWA neurons are involved in attractive responses to a variety of chemicals, we hypothesized that expressing *tyra-2* in AWA neurons would result in attraction to osas#9. To test this, we constructed two different transgenic lines, which mis-express *tyra-2* in the AWA neurons in a *tyra-2 lof* background.

As the avoidance response drop assay tests the animal's acute response to a test compound presented to it briefly, where only avoidance or the lack thereof can be scored, it does not lend itself to assaying attraction. Hence, we designed a simple holding assay that involves the placement of animals into a droplet of solution placed in the center of a NGM agar plate. This assay can measure attraction since the animal can freely move toward or away from the droplet: animals attracted to components in the solution would remain closer to the origin, whereas those repelled would move farther away. We measured the distance of animals from the origin in one-minute intervals (Fig. 4C). As expected, *tyra-2 lof* animals placed in osas#9 droplets displayed leaving rates equal to the solvent control. (Fig. 4D, S4). Notably, worms mis-expressing *tyra-2* in the AWA neurons, when placed into osas#9 droplets, displayed leaving rates lower than that for solvent controls, indicating attraction (Fig. 4D, S4). Furthermore, these worms stayed significantly closer to the origin than both wild-type and *tyra-2 lof* animals when exposed to osas#9 (Fig. 4D, S4). Ectopic expression of *tyra-2* in AWA did not alter either locomotory parameters or normal diacetyl chemotaxis (Fig. S5A,B).

To further investigate the role of *tyra-2* in chemoreception, we measured calcium transients using GCaMP2.2b expressed in AWA neurons in both wild-type and AWA::*tyra-2* animals (Fig. 5E,F). Both lines displayed depolarization in response to diacetyl as previously reported (Fig. S5 D,E), suggesting that the AWA::*tyra-2* line displays normal neuronal dynamics. In contrast, upon osas#9 stimulation, we observed distinct hyperpolarization in AWA::*tyra-2* animals, whereas no change in fluorescence was observed in animals lacking *tyra-2* in AWA neurons (Fig. 4E,F). Given that depolarization of AWA neurons upon diacetyl stimulation results in suppressed turning behavior (50), we asked whether AWA hyperpolarization by osas#9 increases reversals in AWA::*tyra-2* mis-expression animals. Indeed, we found that AWA::*tyra-2* animals reverse

roughly two times as much when exposed to osas#9 compared to *tyra-2* mutant and wild-type animals (Fig. S5C). Our findings suggest that in worms mis-expressing TYRA-2 in the AWA neurons osas#9 perception results in hyperpolarization of this neuron, increasing reversal frequency, resulting in attraction to osas#9.

Discussion

Our data for TYRA-2 indicate that this GPCR is required for osas#9 perception in the ASH sensory neuron. ASH, as a polymodal nociceptive neuron, is involved in many avoidance responses stimulated by mechano-, osmo-, and chemosensation deterrents. To our knowledge this is the first characterized ASH role in pheromone detection (38, 40, 42, 51-60). Although rescue of *osm-9* in ASH alone was enough to reconstitute wild type behavior (Fig. 3B), it appears that other sensory neurons, particularly ASE and ASI may assist in regulating the response (Fig. 3A). Perhaps these neurons are interacting with ASH neurons, in a similar manner to how AWC neurons act as a switch for AIB and AIY interneurons in food odor perception (61). Alternatively, modulation at the sensory level could regulate ASH function, as observed in cross inhibition of ASI and ASH neuronal activity in avoidance to copper (62). It will be interesting to elucidate the role other neurons and peptidergic signaling have in shaping the osas#9 response. Such modulation of the osas#9 response, as well as the effects of physiological state and environmental conditions of the circuitry remain to be investigated.

TYRA-2 has previously been shown to contain the conserved $Asp^{3.32}$ required for amine binding, allowing the receptor to bind tyramine with high affinity as well as octopamine (34). Recent studies have shown that *tyra-2* is necessary for binding tyramine in a RIM-ASH feedback loop in multisensory decision making (63). Animals lacking TYRA-2 or TDC-1 crossed a 3 M fructose barrier towards an attractant, diacetyl, faster than wild-type *C. elegans,* demonstrating the endogenous role of tyramine binding to TYRA-2 in multisensory threat tolerance (31, 63). However, *tyra-2* is not involved in *unisensory* responses to anterior touch, octanol avoidance, feeding rates, paralysis, copper, SDS, or glycerol avoidance (Fig. S1B) (38, 62, 64-66). We have found that *tyra-2* is necessary for *unisensory* avoidance to osas#9, and that this function is independent of endogenous tyramine. Osas#9 is chemically derived from octopamine via succinylation of the free amine and addition of an ascaroside moiety. The octopamine moiety in

the structure osas#9 is fully preserved, suggesting that osas#9 could be a ligand of TYRA-2. Our findings that TYRA-2 is localized in the cilia and that ectopic expression of TYRA-2 in the AWA neuron confers attraction to osas#9, whereas expression of TYRA-2 in ASH results in osas#9 avoidance, further support that the GPCR TYRA-2 directly interacts with osas#9. Characterization of the GPCRs *daf-37* and *daf-38*, which are involved in perception of the dauer pheromone component ascr#2, demonstrated that some *C. elegans* GPCRs involved in pheromone perception act as heterodimers (29). Analogously, TYRA-2 could interact with a different receptor that is expressed in both the ASH and AWA neurons, e.g. forming a heterodimer, to bind osas#9. In either scenario, the avoidance response to osas#9 may be physiologically regulated via TYRA-2 expression levels (Fig. 4B).

Taken together, our findings demonstrate that TYRA-2, a member of a well conserved family of neurotransmitter receptors, functions in chemosensation of osas#9, a neurotransmitter-derived inter-organismal signal. Therefore, it appears that in *C. elegans* the evolution of inter-organismal communication co-opted both a neurotransmitter, octopamine, and the related receptor TYRA-2, for mediating starvation-dependent dispersal. Such co-option of intra-organismal signaling pathways has been hinted at for two other classes of chemoreceptors, the trace amine-associated receptors (TAAR) and formyl peptide receptor-like (FPRL) receptors (67-70). While both receptor classes have a receptor involved in immune system chemotaxis, the evidence for their involvement in olfaction does not go beyond evidence of expression in the vomeronasal organ. Our results demonstrate recruitment of both neurotransmitter biosynthesis and neurotransmitter reception for inter-organismal signaling, suggesting that such co-option of elements of intra-organismal signaling may represent one mechanism for the emergence of new pheromonal communication pathways.

Methods

Drop avoidance test

In this assay, the tail end of a forward moving animal is subjected to a small drop (~5 nl) of solution, delivered through a hand-pulled 10 µl glass capillary tube. The solution, upon contact, is drawn up to the amphid sensory neurons via capillary action. In response, the animal either continues its forward motion (scored as "no avoidance response"), or displays an avoidance response within four seconds (60). The avoidance response is characterized by a reversal consisting of at least one half of a complete "head swing" followed by a change in direction of at least 90 degrees from the original vector. For quantitative analysis, an avoidance response is marked as a "1" and no response as a "0". The avoidance index is calculated by dividing the number of avoidance responses by the total number of trials. Each trial is done concurrently with osas#9 and a solvent control. The fold change is then calculated and the data normalized where wild-type fold change is 100%, and no fold change is 0%.

Integrated mutant strains and controls are prepared using common M9 buffer to wash and transfer a plate of animals to a microcentrifuge tube where the organisms are allowed to settle. The supernatant is removed and the animals are resuspended and allowed to settle again. The supernatant is again removed and the animals then transferred to an unseeded plate. After 1 hour, young adult animals are subjected to the solvent control and the chemical of interest at random with no animal receiving more than one drop of the same solution.

Ablated and extrachromosomal mutant animals and controls are gently passed onto an unseeded plate and allowed to crawl around. They are then gently passed to another unseeded plate to minimalize bacterial transfer. Each animal is tested three times with the solvent control and solution of interest with 2 minute intervals between drops (60).

Strains and Plasmids

tyra-2 rescue and misexpression plasmids were made using MultiSite Gateway Pro Technology and injected into strain FX01846 *tyra-2* (tm1846) with co-injection marker p*elt-2*;mCherry by Knudra Transgenics. The promoter attB inserts were generated using PCR and genomic DNA or a plasmid. The *tyra-2* insert was isolated from genomic DNA using attB5*ggcttatccgttgtggagaa* and

attB2*ttggcccttccttttctctt.* PDONR221 p1-p5r and PDONR221P5-P2 donor vectors were used with attB inserts. The resultant entry clones were used with the destination vector pLR305 and pLR306.

AWA::*tyra-2* misexpression*:* For AWA expression, a 1.2 kb *odr-10* promoter was isolated from genomic DNA using primers attB1*ctcgctaaccactcggtcat* and attB5r*gtcaactagggtaatccacaattc.* Entry clones were used with destination vector pLR305 resulting in p*odr-10::tyra-2:: RFP* and co-injected with p*elt-2*::mCherry into FX01846.

ASH::*tyra-2* rescue*:* For ASH expression, a 3 kb *nhr-79* promoter was isolated from genomic DNA using primers attB1*gtgcaatgcatggaaaattg* and attB5r*atacacttcccacgcaccat.* Entry clones were used with destination vector pLR306 resulting in p*nhr-79::tyra-2::RFP* and co-injected with p*elt-2*::mCherry into FX01846.

Translational fusions*: tyra-2::*gfp fusions were created by PCR fusion using the following primers: A) *atgttttcacaagtttcaccaca,* A nested) *ttcacaagtttcaccacattacaa,* and B with overhang) *AGTCGACCTGCAGGCATGCAAGCT gacacgagaagttgagctgggtttc.* GFP primers as described in WormBook (71). The construct was then co-injected with p*elt-2*::mCherry into both N2 and FX01846. Injections were performed by Knudra Transgenics, Utah and by MA lab.

See Supplementary Table 1-3 for details on strains, plasmids, and primers used in this study.

RNA interference

RNAi knockdown experiments were completed following the Ahringer RNAi feeding protocol found at Source Bioscience (http://www.us.lifesciences.sourcebioscience.com/clone-products/non-mammalian/c-elegans/c-elegans-rnai-library/ahringer-lab-clone-information-and-rnai-feeding-protocol/). The RNAi clones (F01E11.5, F14D12.6, and empty pL4440 vector in HT115) were generously provided by the Ambros Lab at UMASS Medical School, and originated from the Vidal Library (72). We found the RNAi worked best when animals were cultured at 15 ºC. *C. elegans* strain NL3321 *sid-1* (pk3321) were used for the RNAi studies.

Laser ablations

Laser ablations were carried out using DIC optics and the MicroPoint laser system following the procedures as outlined in Fang-Yen *et al.* 2012 (73, 74). Ablated animals were assayed 72 hours

later, at the young adult stage. All ablated animals were tested in parallel with control animals that went through the same process, minus the firing of the laser (also called Mock animals).

Imaging

Translational fusion animals were prepared for imaging by mounting them to a 4% agar pad with 10 mM levamisole on a microscope slide as outlined in O'Hagen and Barr 2016 (75).

Animals for cilia imaging were imaged using a Nikon Multispectral Multimode Spinning Disk Confocal Microscope, courtesy of Dr. Kwonmoo Lee at Worcester Polytechnic Institute.

Animals for measuring cilia fluorescence were imaged at 40x using a Zeiss Apotome microscope. Cilia fluorescence was quantified using ImageJ.

Calcium Imaging was performed by using a modified olfactory chip, and detailed procedural information can be found in *Reilly et al.* (44, 45). Briefly, a young adult animal was immobilized in a PDMS olfactory chip with its nose subject to flowing solution. An animal was imaged at 40x three times for 30 seconds, and experienced a 10 second pulse of osas#9 in between the solvent control. Soma fluorescence from GCaMP3 was measured using imageJ. $\Delta F/F$ was calculated by dividing the fluorescence in the frames of interest by the average fluorescence of ten frames before the stimuli (45).

RT-qPCR

RNA was isolated from individual animals, either freshly removed from food or after four hours of starvation using proteinase K buffer as previously published. (76). cDNA was then synthesized using the Maxima H Minus First Strand cDNA Synthesis Kit. iTaq Universal SYBR Green Supermix was used for amplification with the Applied Biosystem 7500 Real Time system Primer efficiency was determined to be 97.4% for *tyra-2* primers (GAGGAGGAAGAAGATAGCGAAAG, TGTGATCATCTCGCTTTTCA) and 101.8% for the reference gene *ama-1* (GGAGATTAAACGCATGTCAGTG, ATGTCATGCATCTTCCACGA) using the equation 10^(-1/slope)-1. Technical replicates with large standard deviations and trials with a Ct within 5 cycles of the negative control (no reverse transcriptase used in prep) were removed from analyses.

Locomotion

Speed*:* Five animals were gently transferred to a 35mm plate and filmed for 20 minutes. Videos were generated using the Wormtracker system by MBF Bioscience. Videos were then analyzed and average speed computed using the WormLab software built in with the tracker system.

Reversals*:* Reversals were analyzed and measured using Wormlab (MBF Bioscience) from videos recorded for the holding assay between minute one and two as it was when the divergence was first seen in distance between strains in the holding assay.

Chemoattraction

Diacetyl chemotaxis assays were carried out as previously published, with slight modifications (77). Briefly, 10 animals were placed in the center of a 35mm plate, equidistant from two spots of interest, one containing 1 µl of solvent control and the other 1 µl of 10^{-2} diacetyl. Both regions also contained 1 µl of 1 M sodium azide for anesthetizing animals that entered the region. After 45 minutes the chemotaxis index was calculated by subtracting the number of animals in the solvent control from the number of animals in the solution of interest and divided by the total number of animals.

Holding Assay

The holding assay consisted of the use of 60 mm culture plates with standard NGM agar. A transparency template that included a 6mm diameter circle in the center was attached to the underside of the NGM plate. One hour before running the assay young adult animals were passed on to an unseeded plate and 100 µl of *E. coli* op50 liquid culture was spread onto separate NGM assay plates. These plates were allowed to dry at 25°C without a lid. After a one hour incubation, 4 µl of either the solvent control or 10 pM osas#9 was pipetted onto the agar within the center circle outlined on the template. 10 animals were gently passed into the solution and their movement was recorded. At one minute intervals, the distance the animals traveled from the origin was measured using ImageJ. Immobile animals were removed from the data set prior to analysis, as well as statistical outliers (as determined by distances greater than two standard deviations away from the average distance).

Statistical analysis

Statistical tests were run using Graphpad Prism. For all figures, when comparing multiple groups, ANOVAs were performed followed by Sidak's multiple comparison test. When only two groups were compared, a Student's t-test was used (Figure 1B, 4B). When comparing different strains/conditions, normalized values of osas#9 avoidance index response relative to the respective solvent control were used. This was done to account for any differences in the response to solvent control for the respective genotypes, laser ablations or physiological conditions. When normalizing fold change of osas#9 response to solvent control response for the avoidance assay within a strain/condition, data was first log transformed so a fold change could still be calculated for control plates that had a "0" value. For avoidance assays, statistical groups were based on the number of plates assayed, not the number of drops/animals. Calcium imaging statistics were based on pulses and at least 10 animals.

Acknowledgements

We thank the *Caenorhabditis* Genetics Center (CGC), which is funded by the NIH Office of Research Infrastructure Programs (P40 OD010440), R. Komuniecki, S. Suo, D. Chase, V. Ambros, C. Bargmann, and P. Sternberg for strains; R. Garcia, D. Albrecht, and S. Chalasani for plasmids; K. Lee for the use of the labs spinning-disk confocal microscope; V. Ambros, Dana-Farber Cancer Institute, and BioScience Life Sciences for RNAi clones; the Srinivasan lab and S. Chalasani for critical comments on the manuscript; A. Warty for contribution to glycerol assays. This work was supported in by grants from the NIH (R01DC016058 to J.S. and GM113692 and GM088290 to FCS), and startup funds from WPI.

Author Contributions

CDC performed the molecular biology, ablations, imaging, and behavioral assays. VC Performed the RNAi behavioral assays. YZ synthesized osas#9. H. Choi imaged fusion lines. DR generated strains from MA lab. CDC, MA, FCS, and JS wrote the manuscript.

1. Chase DL, Koelle MR. Biogenic amine neurotransmitters in *C. elegans*. WormBook : the online review of *C. elegans* biology. 2007:1-15.
2. Artyukhin AB, Yim JJ, Srinivasan J, Izrayelit Y, Bose N, von Reuss SH, et al. Succinylated octopamine ascarosides and a new pathway of biogenic amine metabolism in *Caenorhabditis elegans*. J Biol Chem. 2013;288(26):18778-83.
3. von Reuss SH, Schroeder FC. Combinatorial chemistry in nematodes: modular assembly of primary metabolism-derived building blocks. Natural product reports. 2015;32(7):994-1006.
4. Slobodchikoff CN, Paseka A, Verdolin JL. Prairie dog alarm calls encode labels about predator colors. Animal cognition. 2009;12(3):435-9.
5. Barske J, Schlinger BA, Wikelski M, Fusani L. Female choice for male motor skills. Proceedings Biological sciences / The Royal Society. 2011;278(1724):3523-8.
6. Riley JR, Greggers U, Smith AD, Reynolds DR, Menzel R. The flight paths of honeybees recruited by the waggle dance. Nature. 2005;435(7039):205-7.
7. Waters CM, Bassler BL. Quorum sensing: cell-to-cell communication in bacteria. Annual review of cell and developmental biology. 2005;21:319-46.
8. Guerrieri E, Poppy GM, Powell W, Rao R, Pennacchio F. Plant-to-plant communication mediating in-flight orientation of Aphidius ervi. Journal of chemical ecology. 2002;28(9):1703-15.
9. Kunert G, Otto S, Röse USR, Gershenzon J, Weisser WW. Alarm pheromone mediates production of winged dispersal morphs in aphids. Ecology Letters. 2005;8(6):596-603.
10. Akiyama K, Matsuzaki K, Hayashi H. Plant sesquiterpenes induce hyphal branching in arbuscular mycorrhizal fungi. Nature. 2005;435(7043):824-7.
11. Roschina VV. Evolutionary considerations of neurotransmitters in microbial, plant, and animal cells. microbial endocrnology: springer new york; 2010. p. 17-52.
12. Krishnan A, Schioth HB. The role of G protein-coupled receptors in the early evolution of neurotransmission and the nervous system. The Journal of experimental biology. 2015;218(Pt 4):562-71.
13. Tecott LH. Serotonin and the orchestration of energy balance. Cell metabolism. 2007;6(5):352-61.
14. Roeder T. Tyramine and octopamine: ruling behavior and metabolism. Annu Rev Entomol. 2005;50:447-77.
15. Bargmann CI. Neurobiology of the *Caenorhabditis elegans* genome. Science. 1998;282(5396):2028-33.
16. White JG, Southgate E, Thomson JN, Brenner S. The structure of the nervous system of the nematode *Caenorhabditis elegans*. Philosophical transactions of the Royal Society of London Series B, Biological sciences. 1986;314(1165):1-340.
17. Chute CD, Srinivasan J. Chemical mating cues in *C. elegans*. Seminars in cell & developmental biology. 2014;33:18-24.
18. Srinivasan J, Kaplan F, Ajredini R, Zachariah C, Alborn HT, Teal PEA, et al. A blend of small molecules regulates both mating and development in *Caenorhabditis elegans*. Nature. 2008;454(7208):1115-8.
19. Schroeder FC. Modular assembly of primary metabolic building blocks: a chemical language in *C. elegans*. Chem Biol. 2015;22(1):7-16.
20. Kaplan F, Srinivasan J, Mahanti P, Ajredini R, Durak O, Nimalendran R, et al. Ascaroside expression in *Caenorhabditis elegans* is strongly dependent on diet and developmental stage. PloS one. 2011;6(3):e17804.

21. Butcher RA, Ragains JR, Kim E, Clardy J. A potent dauer pheromone component in *Caenorhabditis elegans* that acts synergistically with other components. Proceedings of the National Academy of Sciences of the United States of America. 2008;105(38):14288-92.
22. Jeong PY, Jung M, Yim YH, Kim H, Park M, Hong E, et al. Chemical structure and biological activity of the *Caenorhabditis elegans* dauer-inducing pheromone. Nature. 2005;433(7025):541-5.
23. Srinivasan J, Kaplan F, Ajredini R, Zachariah C, Alborn HT, Teal PE, et al. A blend of small molecules regulates both mating and development in *Caenorhabditis elegans*. Nature. 2008;454(7208):1115-8.
24. Butcher RA, Fujita M, Schroeder FC, Clardy J. Small-molecule pheromones that control dauer development in *Caenorhabditis elegans*. nature chemical biology. 2007;3(7):420-2.
25. Pungaliya C, Srinivasan J, Fox BW, Malik RU, Ludewig AH, Sternberg PW, et al. A shortcut to identifying small molecule signals that regulate behavior and development in *Caenorhabditis elegans*. Proceedings of the National Academy of Sciences of the United States of America. 2009;106(19):7708-13.
26. Greene JS, Brown M, Dobosiewicz M, Ishida IG, Macosko EZ, Zhang X, et al. Balancing selection shapes density-dependent foraging behaviour. Nature. 2016;539(7628):254-8.
27. Greene JS, Dobosiewicz M, Butcher RA, McGrath PT, Bargmann CI. Regulatory changes in two chemoreceptor genes contribute to a *Caenorhabditis elegans* QTL for foraging behavior. eLife. 2016;5.
28. McGrath PT, Xu Y, Ailion M, Garrison JL, Butcher RA, Bargmann CI. Parallel evolution of domesticated *Caenorhabditis* species targets pheromone receptor genes. Nature. 2011;477(7364):321-5.
29. Park D, O'Doherty I, Somvanshi RK, Bethke A, Schroeder FC, Kumar U, et al. Interaction of structure-specific and promiscuous G-protein-coupled receptors mediates small-molecule signaling in *Caenorhabditis elegans*. Proceedings of the National Academy of Sciences of the United States of America. 2012;109(25):9917-22.
30. Kim K, Sato K, Shibuya M, Zeiger DM, Butcher RA, Ragains JR, et al. Two chemoreceptors mediate developmental effects of dauer pheromone in *C. elegans*. Science. 2009;326(5955):994-8.
31. Alkema MJ, Hunter-Ensor M, Ringstad N, Horvitz HR. Tyramine Functions independently of octopamine in the *Caenorhabditis elegans* nervous system. Neuron. 2005;46(2):247-60.
32. Narayan A, Venkatachalam V, Durak O, Reilly DK, Bose N, Schroeder FC, et al. Contrasting responses within a single neuron class enable sex-specific attraction in *Caenorhabditis elegans*. Proceedings of the National Academy of Sciences of the United States of America. 2016;113(10):E1392-401.
33. Srinivasan J, von Reuss SH, Bose N, Zaslaver A, Mahanti P, Ho MC, et al. A modular library of small molecule signals regulates social behaviors in *Caenorhabditis elegans*. PLoS biology. 2012;10(1):e1001237.
34. Rex E, Hapiak V, Hobson R, Smith K, Xiao H, Komuniecki R. TYRA-2 (F01E11.5): a *Caenorhabditis elegans* tyramine receptor expressed in the MC and NSM pharyngeal neurons. Journal of neurochemistry. 2005;94(1):181-91.
35. Rex E, Komuniecki RW. Characterization of a tyramine receptor from *Caenorhabditis elegans*. Journal of neurochemistry. 2002;82(6):1352-9.
36. Suo S, Kimura Y, Van Tol HH. Starvation induces cAMP response element-binding protein-dependent gene expression through octopamine-Gq signaling in *Caenorhabditis elegans*.

The Journal of neuroscience : the official journal of the Society for Neuroscience. 2006;26(40):10082-90.
37. Mills H, Wragg R, Hapiak V, Castelletto M, Zahratka J, Harris G, et al. Monoamines and neuropeptides interact to inhibit aversive behaviour in *Caenorhabditis elegans*. The EMBO journal. 2012;31(3):667-78.
38. Wragg RT, Hapiak V, Miller SB, Harris GP, Gray J, Komuniecki PR, et al. Tyramine and octopamine independently inhibit serotonin-stimulated aversive behaviors in *Caenorhabditis elegans* through two novel amine receptors. The Journal of neuroscience : the official journal of the Society for Neuroscience. 2007;27(49):13402-12.
39. Colbert HA, Smith TL, Bargmann CI. OSM-9, a novel protein with structural similarity to channels, is required for olfaction, mechanosensation, and olfactory adaptation in *Caenorhabditis elegans*. The Journal of neuroscience : the official journal of the Society for Neuroscience. 1997;17(21):8259-69.
40. de Bono M, Tobin DM, Davis MW, Avery L, Bargmann CI. Social feeding in *Caenorhabditis elegans* is induced by neurons that detect aversive stimuli. Nature. 2002;419(6910):899-903.
41. Liedtke W, Tobin DM, Bargmann CI, Friedman JM. Mammalian TRPV4 (VR-OAC) directs behavioral responses to osmotic and mechanical stimuli in *Caenorhabditis elegans*. Proceedings of the National Academy of Sciences of the United States of America. 2003;100 Suppl 2:14531-6.
42. Hilliard MA, Bergamasco C, Arbucci S, Plasterk RH, Bazzicalupo P. Worms taste bitter: ASH neurons, QUI-1, GPA-3 and ODR-3 mediate quinine avoidance in *Caenorhabditis elegans*. The EMBO journal. 2004;23(5):1101-11.
43. Miyabayashi T, Palfreyman MT, Sluder AE, Slack F, Sengupta P. Expression and function of members of a divergent nuclear receptor family in *Caenorhabditis elegans*. Dev Biol. 1999;215(2):314-31.
44. Chronis N, Zimmer M, Bargmann CI. Microfluidics for in vivo imaging of neuronal and behavioral activity in *Caenorhabditis elegans*. Nature methods. 2007;4(9):727-31.
45. Douglas K. Reilly Daniel E. Lawler, Dirk R. Albrecht, Jagan Srinivasan. Using an Adapted Microfluidic Olfactory Chip for the Imaging of Neuronal Activity in Response to Pheromones in Male *C. elegans* Head Neurons. JOVE. In Press.
46. Ryan DA, Miller RM, Lee K, Neal SJ, Fagan KA, Sengupta P, et al. Sex, age, and hunger regulate behavioral prioritization through dynamic modulation of chemoreceptor expression. Current biology : CB. 2014;24(21):2509-17.
47. Gruner M, Nelson D, Winbush A, Hintz R, Ryu L, Chung SH, et al. Feeding state, insulin and NPR-1 modulate chemoreceptor gene expression via integration of sensory and circuit inputs. PLoS genetics. 2014;10(10):e1004707.
48. Fox AN, Pitts RJ, Robertson HM, Carlson JR, Zwiebel LJ. Candidate odorant receptors from the malaria vector mosquito Anopheles gambiae and evidence of down-regulation in response to blood feeding. Proceedings of the National Academy of Sciences of the United States of America. 2001;98(25):14693-7.
49. Troemel ER, Kimmel BE, Bargmann CI. Reprogramming chemotaxis responses: sensory neurons define olfactory preferences in *C. elegans*. Cell. 1997;91(2):161-9.
50. Larsch J, Flavell SW, Liu Q, Gordus A, Albrecht DR, Bargmann CI. A Circuit for Gradient Climbing in *C. elegans* Chemotaxis. Cell reports. 2015;12(11):1748-60.

51. Campbell JC, Chin-Sang ID, Bendena WG. Mechanosensation circuitry in *Caenorhabditis elegans*: A focus on gentle touch. Peptides. 2015;68:164-74.
52. Hart AC, Kass J, Shapiro JE, Kaplan JM. Distinct signaling pathways mediate touch and osmosensory responses in a polymodal sensory neuron. The Journal of neuroscience : the official journal of the Society for Neuroscience. 1999;19(6):1952-8.
53. Hart AC, Sims S, Kaplan JM. Synaptic code for sensory modalities revealed by *C. elegans* GLR-1 glutamate receptor. Nature. 1995;378(6552):82-5.
54. Kaplan JM, Horvitz HR. A dual mechanosensory and chemosensory neuron in *Caenorhabditis elegans*. Proceedings of the National Academy of Sciences of the United States of America. 1993;90(6):2227-31.
55. Kato S, Xu Y, Cho CE, Abbott LF, Bargmann CI. Temporal responses of *C. elegans* chemosensory neurons are preserved in behavioral dynamics. Neuron. 2014;81(3):616-28.
56. Krzyzanowski MC, Brueggemann C, Ezak MJ, Wood JF, Michaels KL, Jackson CA, et al. The *C. elegans* cGMP-dependent protein kinase EGL-4 regulates nociceptive behavioral sensitivity. PLoS genetics. 2013;9(7):e1003619.
57. Krzyzanowski MC, Woldemariam S, Wood JF, Chaubey AH, Brueggemann C, Bowitch A, et al. Aversive Behavior in the Nematode *C. elegans* Is Modulated by cGMP and a Neuronal Gap Junction Network. PLoS genetics. 2016;12(7):e1006153.
58. Harris G, Mills H, Wragg R, Hapiak V, Castelletto M, Korchnak A, et al. The monoaminergic modulation of sensory-mediated aversive responses in *Caenorhabditis elegans* requires glutamatergic/peptidergic cotransmission. The Journal of neuroscience : the official journal of the Society for Neuroscience. 2010;30(23):7889-99.
59. Hapiak V, Summers P, Ortega A, Law WJ, Stein A, Komuniecki R. Neuropeptides amplify and focus the monoaminergic inhibition of nociception in *Caenorhabditis elegans*. The Journal of neuroscience : the official journal of the Society for Neuroscience. 2013;33(35):14107-16.
60. Hilliard MA, Bargmann CI, Bazzicalupo P. *C. elegans* responds to chemical repellents by integrating sensory inputs from the head and the tail. Current biology : CB. 2002;12(9):730-4.
61. Chalasani SH, Chronis N, Tsunozaki M, Gray JM, Ramot D, Goodman MB, et al. Dissecting a circuit for olfactory behaviour in *Caenorhabditis elegans*. Nature. 2007;450(7166):63-70.
62. Guo M, Wu TH, Song YX, Ge MH, Su CM, Niu WP, et al. Reciprocal inhibition between sensory ASH and ASI neurons modulates nociception and avoidance in *Caenorhabditis elegans*. Nature communications. 2015;6:5655.
63. Ghosh DD, Sanders T, Hong S, McCurdy LY, Chase DL, Cohen N, et al. Neural Architecture of Hunger-Dependent Multisensory Decision Making in *C. elegans*. Neuron. 2016;92(5):1049-62.
64. Pirri JK, McPherson AD, Donnelly JL, Francis MM, Alkema MJ. A tyramine-gated chloride channel coordinates distinct motor programs of a *Caenorhabditis elegans* escape response. Neuron. 2009;62(4):526-38.
65. Greer ER, Perez CL, Van Gilst MR, Lee BH, Ashrafi K. Neural and molecular dissection of a *C. elegans* sensory circuit that regulates fat and feeding. Cell metabolism. 2008;8(2):118-31.
66. Donnelly JL, Clark CM, Leifer AM, Pirri JK, Haburcak M, Francis MM, et al. Monoaminergic orchestration of motor programs in a complex *C. elegans* behavior. PLoS biology. 2013;11(4):e1001529.
67. Liberles SD, Buck LB. A second class of chemosensory receptors in the olfactory epithelium. Nature. 2006;442(7103):645-50.

68. Babusyte A, Kotthoff M, Fiedler J, Krautwurst D. Biogenic amines activate blood leukocytes via trace amine-associated receptors TAAR1 and TAAR2. Journal of leukocyte biology. 2013;93(3):387-94.
69. Riviere S, Challet L, Fluegge D, Spehr M, Rodriguez I. Formyl peptide receptor-like proteins are a novel family of vomeronasal chemosensors. Nature. 2009;459(7246):574-7.
70. Stempel H, Jung M, Perez-Gomez A, Leinders-Zufall T, Zufall F, Bufe B. Strain-specific Loss of Formyl Peptide Receptor 3 in the Murine Vomeronasal and Immune Systems. J Biol Chem. 2016;291(18):9762-75.
71. Boulin T, Etchberger JF, Hobert O. Reporter gene fusions. WormBook : the online review of C elegans biology. 2006:1-23.
72. Rual JF, Ceron J, Koreth J, Hao T, Nicot AS, Hirozane-Kishikawa T, et al. Toward improving *Caenorhabditis elegans* phenome mapping with an ORFeome-based RNAi library. Genome research. 2004;14(10B):2162-8.
73. Fang-Yen C, Gabel CV, Samuel AD, Bargmann CI, Avery L. Laser microsurgery in *Caenorhabditis elegans*. Methods in cell biology. 2012;107:177-206.
74. Srinivasan J, Durak O, Sternberg PW. Evolution of a polymodal sensory response network. BMC biology. 2008;6:52.
75. O'Hagan R, Barr MM. Kymographic Analysis of Transport in an Individual Neuronal Sensory Cilium in *Caenorhabditis elegans*. Methods in molecular biology. 2016;1454:107-22.
76. Ly K, Reid SJ, Snell RG. Rapid RNA analysis of individual *Caenorhabditis elegans*. MethodsX. 2015;2:59-63.
77. Bargmann CI, Hartwieg E, Horvitz HR. Odorant-selective genes and neurons mediate olfaction in *C. elegans*. Cell. 1993;74(3):515-27.

Figure 1. osas#9 serves as a dispersal cue. **A)** Structure and functional variation of ascarosides. Octopamine succinylated ascaroside #9 (osas#9) is involved in avoidance. Indole ascaroside #3 (icas#3) attracts hermaphrodites. Ascaroside #8 (ascr#8) attracts males at low concentrations and induces dauer formation at high concentrations. **B)** Animals avoid osas#9. Avoidance index (AI=number of avoidance responses / by total responses in drop avoidance test assay) for young adult (YA) wild-type (N2) animals in response to the solvent control (SC) and to 1 μM osas#9, n=8. **C)** All life stages and males respond to 1 μM osas#9. All other assays were performed on YA animals, n≥4. **D)** osas#9 exhibits avoidance response over a broad range of concentrations in YA wild-type animals. 1.0 μM osas#9 is noted as it the concentration used in all other assays unless noted otherwise, n≥3. **E)** Physiological state affects osas#9 response. Only starved animals respond significantly different to 1 μM osas#9 when compared to solvent control, n≥3. **F)** Working model of ecological role of osas#9 in *C. elegans* life cycle. An animal navigating its environment encounters a food source and offspring grow and reproduce eventually depleting food. Eggs hatch on depleted food patch and L1 arrest animals develop, secreting osas#9. This assists in dispersal away from unfavorable conditions. Data presented as mean ± S.E.M; *P<0.05, **P<0.01, ***P<0.001, ****P<0.0001. Asterisks displayed depict compared osas#9 avoidance response to the solvent control.

Figure 2. *tyra-2* is required for osas#9 aversion. **A)** Tyramine and octopamine receptor screen. *tyra-2 lof* animals are defective in 1μM osas#9 avoidance response, n≥4. **B)** Rescuing *tyra-2* restores wildtype behavior. Using 2kb upstream of the *tyra-2* gene as a promoter, *tyra-2p::*TYRA-2::GFP in a *tyra-2 lof* background reconstituted wild-type behavior to osas#9, n≥5 **C)** osas#9 response is not dependent on tyramine. t*dc-1* mutants, which lack tyramine, show normal response to osas#9, n≥4. **D)** *tyra*-2::GFP translational fusion. *tyra-2* expression was observed in sensory neurons ASE, ASG, ASH, ASH, and NSM. Note that the ASG pair is seen. Strong fluorescence is present in the nerve ring. Image taken at 40x. Data presented as mean ± S.E.M; *P<0.05, **P<0.01, ***P<0.001, ****P<0.0001. Asterisks displayed without bar depict compared 1 μM osas#9 (unless otherwise noted) avoidance response to the solvent control (SC). Asterisks displayed with bar depict compared osas#9 avoidance responses between two different strains/conditions.

Figure 3. *tyra-2* expression in ASH is required for osas#9 behavioral response. **A)** Chemosensory neurons required for osas#9 response. Neurons expressing *tyra-2* were laser ablated. ASH neurons exhibited primary role as an abolished response to osas#9 that was indistinguishable from solvent control and statistically different from mock animals, n≥3. **B)** ASH requires OSM-9 for osas#9 response. OMS-9 rescue in ASH neurons are sufficient to reconstitute wild-type behavior in response to 1 μM osas#9, n≥4. **C)** Confocal image of p*nhr-79*::*tyra-2*::RFP in a *tyra-2 lof* background animal. ASH and ADL neural body pairs can be seen, with processes entering the nerve ring and extending to the tip of the animal at 40x magnification. *tyra-2* is not natively expressed in ADL. **D)** *tyra-2* rescued in ASH neurons fully reconstituted wildtype behavioral response to osas#9. Rescued animals were not statistically different than wild-type animals in their response to 1 μM osas#9, whereas background animals for the rescue lines (*tyra-2 lof*) were. To account for the addition of *tyra-2* expression in ADL, rescue line animals were subjected to ADL

laser ablation, n≥4. **E,F)** Calcium dynamics of ASH neurons upon osas#9 exposure. **E)** ASH::GCaMP3 animals (black) show a change in calcium transients when exposed to osas#9 in a microfluidic olfactory chip. *tyra-2 lof* ASH::GCaMP3 (red) animals did not display a change in fluorescence upon stimulation. Shaded blue region depicts time when animals were subjected to the stimulus, n=10 animals. **F)** Maximum peak fluorescence before (solvent control) and during exposure to 1 μM osas#9 was plotted from the data shown in A for statistical comparison. Without *tyra-2,* no change in calcium transients is seen in ASH, n=10 animals. Data presented as mean ± S.E.M; *P<0.05, **P<0.01, ***P<0.001, ****P<0.0001, n.s.=not significant. Asterisks displayed without bar depict compared 1 μM osas#9 (unless otherwise noted) avoidance response to the solvent control (SC). Asterisks displayed with bar depict compared osas#9 avoidance responses between two different strains/conditions.

Figure 4. Reprogramming AWA sensory neurons switches behavioral response from avoidance to attraction. **A)** Subcellular localization of TYRA-2. 100x confocal image of a *tyra-2*::GFP translational fusion in *tyra-2 lof* showed localization to both the soma and the cilia of the sensory cilia. **B)** RT-qPCR analysis of fed versus starved animals. Starved animals upregulate *tyra-2* nearly two-fold. Data shown is the ratio of endogenous *tyra-2* message to *ama-1* message from three independent RT-qPCR experiments, n=3. **C)** Depiction of the holding assay developed to measure osas#9 attraction. Briefly, animals were placed in the center of a 6 mm diameter ring in 4 μL of solution. Animals were recorded and their distance from the ring measured in mm. **D)** Wild-type, *tyra-2 lof,* and AWA::*tyra-2* lines were subjected to 10 pM osas#9 in the holding assay. The animals' distance was measured from the ring (mm) at minute intervals for 5 minutes. Wild-type animals left the solution of osas#9 quicker than the *tyra-2 lof animals,* whereas the misexpression lines remained closer to osas#9, n≥3. **E,F)** Calcium dynamics of AWA neurons upon osas#9 exposure. **E)** AWA::*tyra-2*::GCaMP2.2b animals (red) show hyperpolarization when exposed to 1 μM osas#9 in a microfluidic olfactory chip. AWA::GCaMP2.2b animals (black) did not display a change in fluorescence upon stimulation. Shaded blue region depicts time when animals were subjected to the stimulus, n=10 animals. **F)** Maximum peak fluorescence before (solvent control) and during exposure to 1 μM osas#9 was plotted from the data shown in E for statistical comparison. Without *tyra-2,* no change in calcium transients is seen in AWA, n=10 animals. Data presented as mean ± S.E.M; *P<0.05, **P<0.01, ***P<0.001, ****P<0.0001, n.s.=not significant. Asterisks displayed without bar depict compared 1 μM osas#9 (unless otherwise noted) avoidance response to the solvent control (SC). Asterisks displayed with bar depict compared osas#9 avoidance responses between two different strains/conditions.

Figure S1. A) Whole body *tyra-2* RNAi knockdown. *sid-1* animals fed with *tyra-2* RNAi construct displayed abnormal osas#9 avoidance response, n≥3. **B)**Wild-type and *tyra-2* subjected to known avoidance inducing solutions. *tyra-2 lof mutants* did not respond statistically differently than wild-type to any solutions tested, n≥3. Data presented as mean ± S.E.M; ****P<0.0001. Asterisks depict comparison between test solution and respective solvent control.

Figure S2. Wild-type animals with ablated neuronal pairs subjected to 1 μM osas#9. Only ASH$^-$ differed statistically from the Mock ablated animals in response to osas#9 and was not statistically different than the solvent control, n≥2. Data presented as mean ± S.E.M; *P<0.05, **P<0.01, ***P<0.001, ****P<0.0001. Asterisks displayed without bar depict compared osas#9 avoidance response to the solvent control. Asterisks displayed with bar depict compared osas#9 avoidance responses between different ablations.

Figure S3. Tyramine and octopamine elicit avoidance at high concentrations. **A,B)** Animals avoid 100 μM and 1 mM octopamine, respectively. Avoidance to high levels of octopamine are independent of *tyra-2*, n≥3. **C,D)** Animals avoid 100 μM and 1 mM tyramine, respectively. Avoidance to high concentrations of tyramine require *tyra-2* in ASH. This further supports the cilia localization imaging and the role of *tyra-2* in being capable of eliciting avoidance behavior, n≥3. **E)** At 1 μM concentrations, animals only avoid osas#9. This implies that *tyra-2*, potentially acting as a heterodimer, is more sensitive to osas#9 than tyramine, n≥3. Data presented as mean ± S.E.M; *P<0.05, **P<0.01, ****P<0.0001. Asterisks depict compared solution of interest avoidance response to the solvent control.

Figure S4. Solvent controls and 10 pM osas#9 for strains in holding assay. **A)** Wild-type, n≥3. **B)** *tyra-2*, n=6. **C)** AWA::*tyra-2* line 1 response to osas#9 differs from its solvent control, n≥6. **D)** AWA::*tyra-2* line 2 response to osas#9 differs from its solvent control, n≥7. **E)** Comparison of solvent control for all strains in holding assay. None of the animals varied in their response, n≥3. Data presented as mean ± S.E.M; *P<0.05.

Figure S5. Expression of *tyra-2* in AWA neurons does not alter native AWA behaviors. **A)** Chemotaxis to 10^{-2} diacetly was unaffected by AWA::*tyra-2,* n≥7. **B)** Locomotory behaviors were unaltered in AWA::*tyra-2* animals. Wild-type, *tyra-2 lof*, and AWA::*tyra-2* speeds are not statistically different, n≥3. **C)** AWA::*tyra-2* animals have an increased reversal rate in comparison to both wild-type and *tyra-2 lof* animals in 10 pM osas#9, n≥3. **D,E)** Calcium dynamics of AWA neurons upon diacetyl exposure **D)** AWA::GCaMP2.2b animals (black) and AWA::*tyra-2*::GCaMP2.2b animals (red) show depolarization when exposed to 10^{-2} diacetyl in a microfluidic olfactory chip.. Shaded blue region depicts time when animals were subjected to the stimulus, n≥8 animals. **E)** Maximum peak fluorescence before (solvent control) and during exposure to 10^{-2} diacetyl was plotted from the data shown in E for statistical comparison, n≥8 animals. Data presented as mean ± S.E.M; *P<0.05, **P<0.01, ****P<0.0001. Asterisks displayed without bar depict compared osas#9 avoidance response to the solvent control. Asterisks displayed with bar depict compared osas#9 avoidance responses between different lines.

Video S1. Video recording of ASH::GCaMP3 animal being stimulated with 1 μM osas#9. osas#9 presented to animal when red dot appears on screen. Blue is low level of fluorescence and red is high fluorescence level.

Table S1. List of Strains

Table S2. List of Plasmids

Table S3. List of Primers

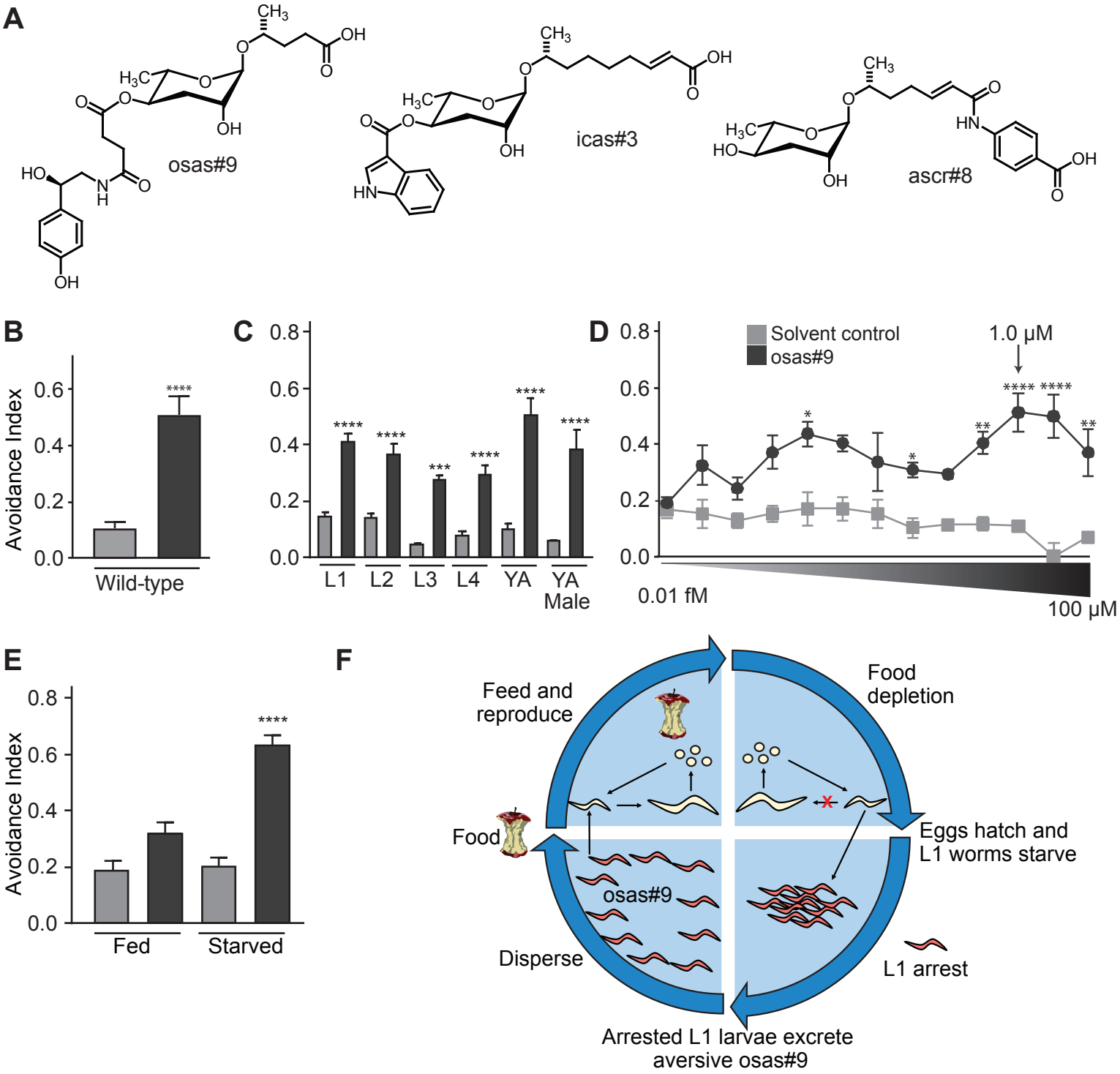
A
osas#9
icas#3
ascr#8
B
Avoidance Index
Wild-type
C
L1
L2
L3
L4
YA
YA Male
D
Solvent control
osas#9
1.0 μM
0.01 fM
100 μM
E
Avoidance Index
Fed
Starved
F
Feed and reproduce
Food depletion
Food
Eggs hatch and L1 worms starve
osas#9
Disperse
L1 arrest
Arrested L1 larvae excrete aversive osas#9

Figure 1

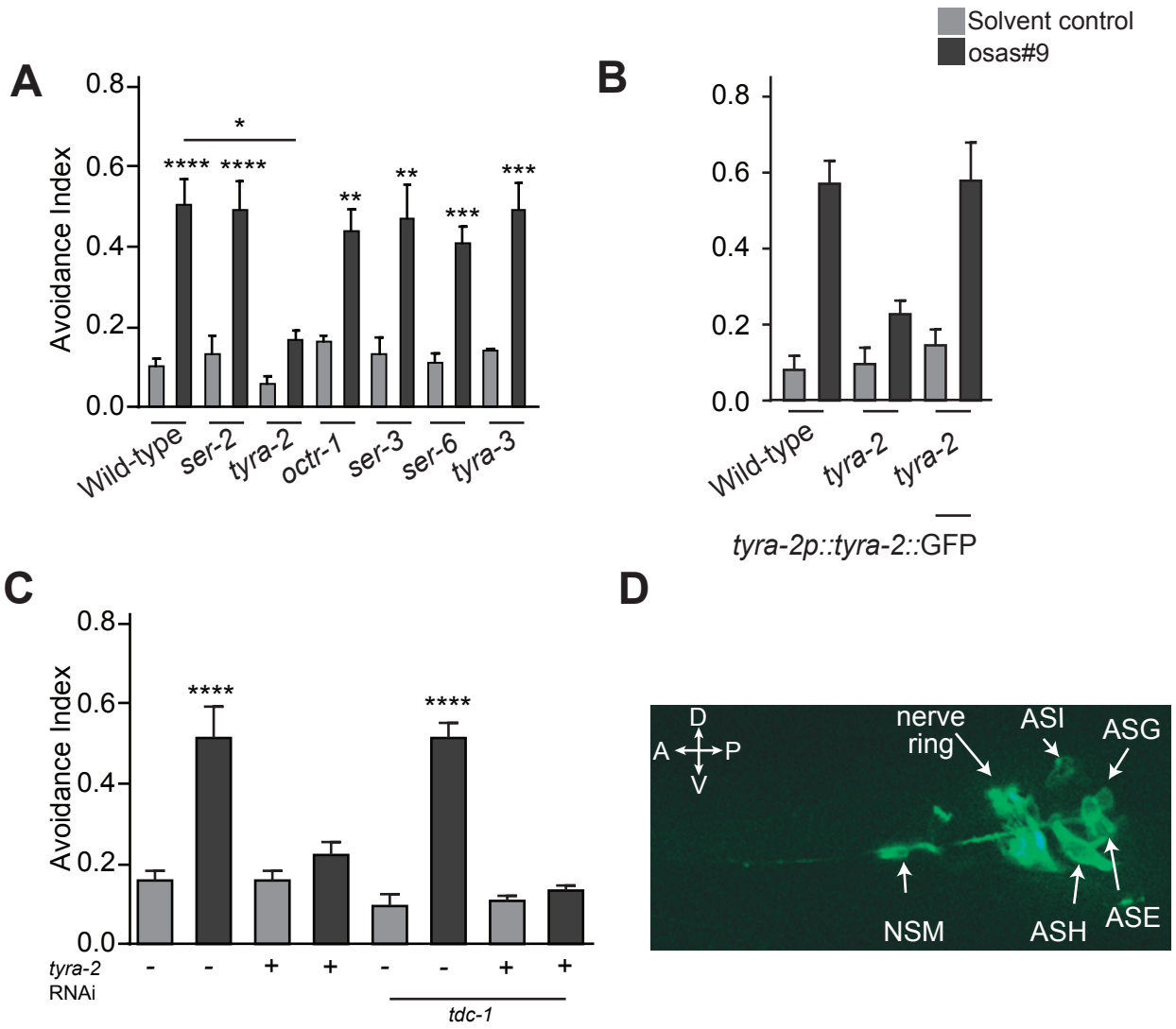
A
Avoidance Index
0.8
0.6
0.4
0.2
0.0
*
****
****
**
**
***
***
Wild-type
ser-2
tyra-2
octr-1
ser-3
ser-6
tyra-3
B
Solvent control
osas#9
0.8
0.6
0.4
0.2
0.0
Wild-type
tyra-2
tyra-2
tyra-2p::tyra-2::GFP
C
Avoidance Index
0.8
0.6
0.4
0.2
0.0
****
****
tyra-2 RNAi
- - + + - - + +
tdc-1
D
D
A
P
V
nerve ring
ASI
ASG
NSM
ASH
ASE

Figure 2

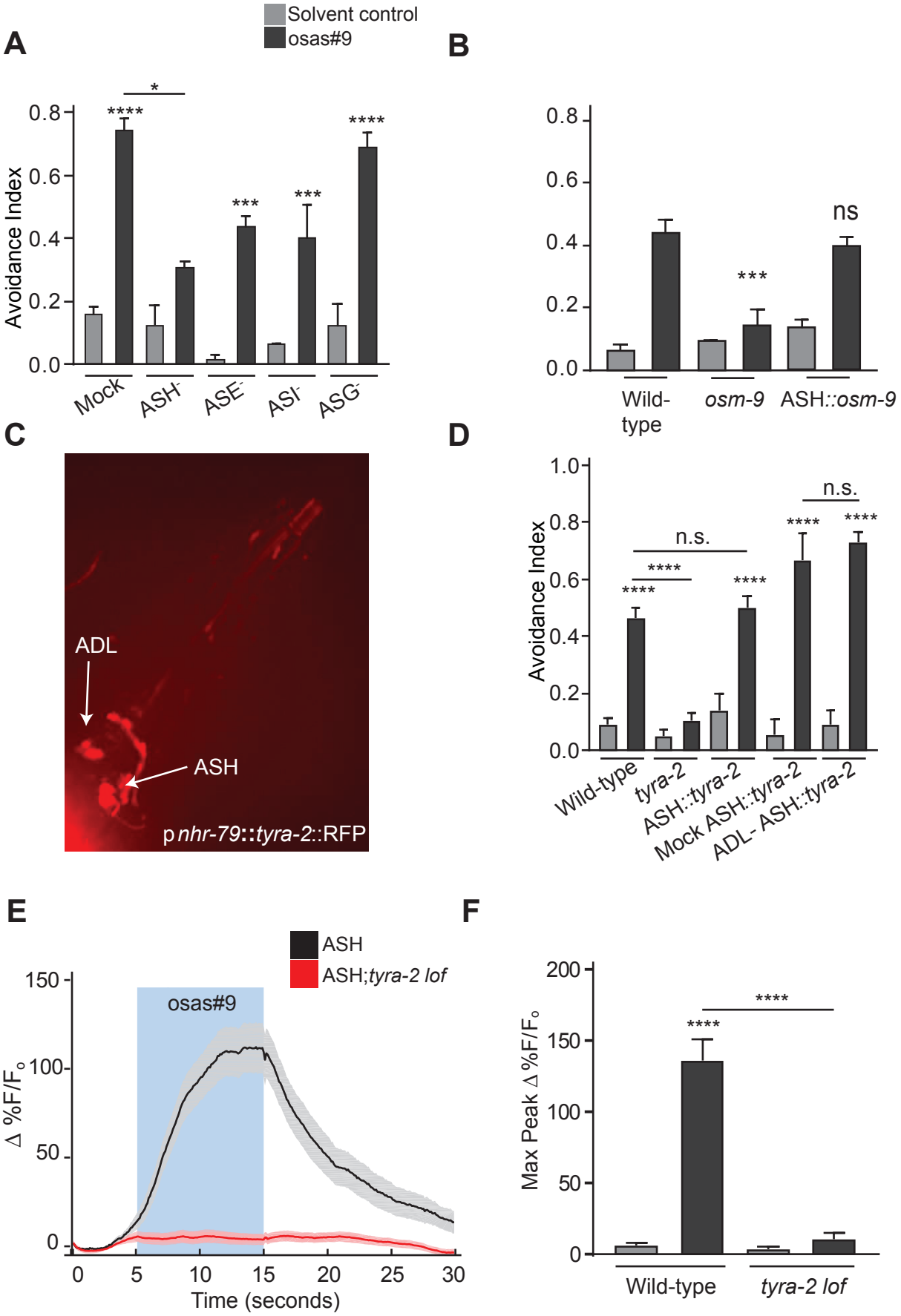
A
Solvent control
osas#9
Avoidance Index
0.8
0.6
0.4
0.2
0.0
*
****
***
***
****
Mock
ASH-
ASE-
ASI-
ASG-
B
0.8
0.6
0.4
0.2
0.0
***
ns
Wild-type
osm-9
ASH::osm-9
C
ADL
ASH
p nhr-79::tyra-2::RFP
D
Avoidance Index
1.0
0.8
0.6
0.4
0.2
0.0
n.s.
n.s.
****
****
****
****
****
Wild-type
tyra-2
ASH::tyra-2
Mock ASH::tyra-2
ADL- ASH::tyra-2
E
ASH
ASH;tyra-2 lof
osas#9
Δ %F/F0
150
100
50
0
0
5
10
15
20
25
30
Time (seconds)
F
Max Peak Δ %F/F0
200
150
100
50
0
****
****
Wild-type
tyra-2 lof

Figure 3

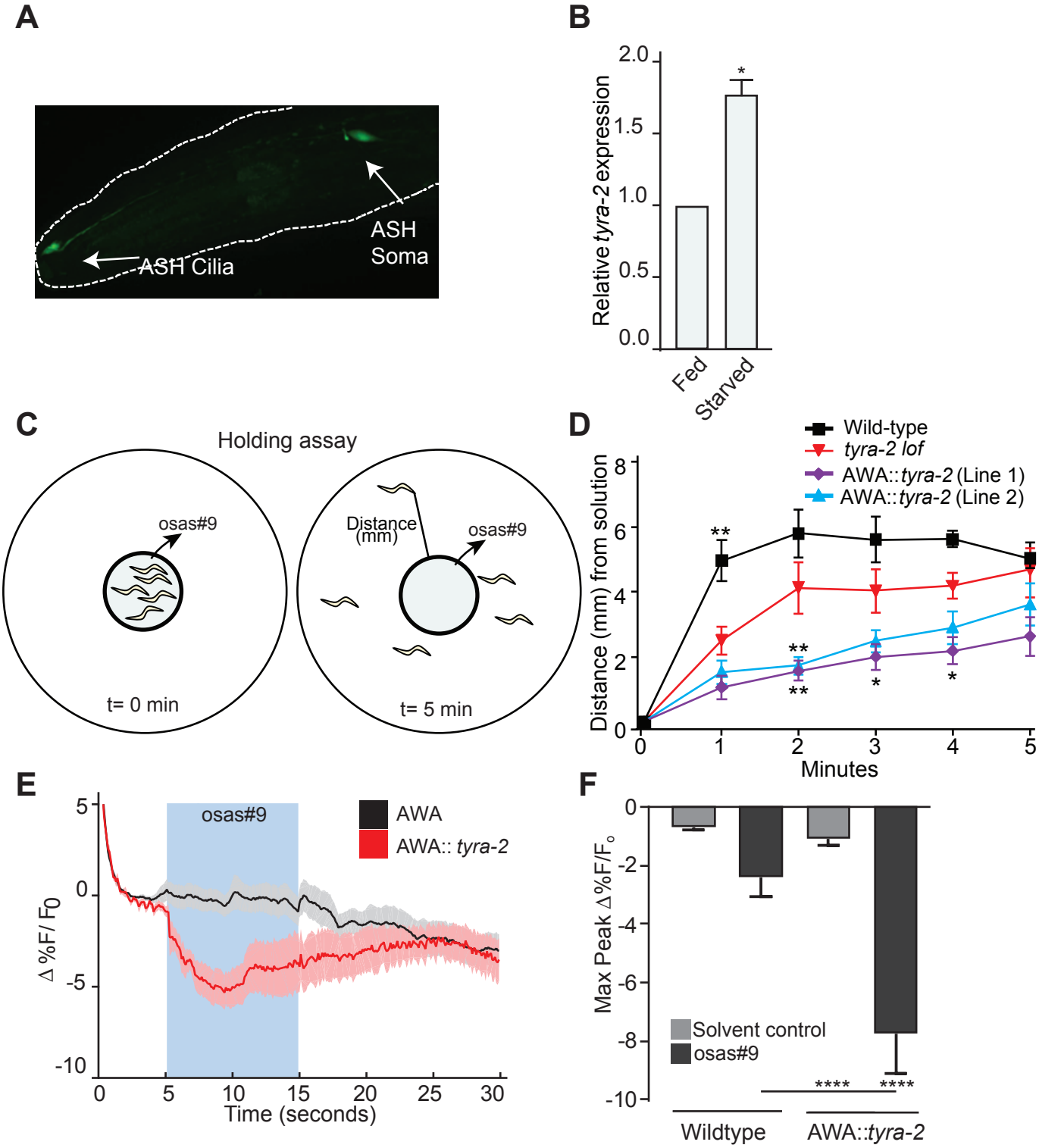
A
ASH Cilia
ASH Soma
B
Relative tyra-2 expression
2.0
1.5
1.0
0.5
0.0
*
Fed
Starved
C
Holding assay
osas#9
t= 0 min
Distance (mm)
osas#9
t= 5 min
D
Wild-type
tyra-2 lof
AWA::tyra-2 (Line 1)
AWA::tyra-2 (Line 2)
Distance (mm) from solution
Minutes
E
osas#9
AWA
AWA:: tyra-2
Δ %F/ F0
Time (seconds)
F
Max Peak Δ%F/F0
Solvent control
osas#9
****
****
Wildtype
AWA::tyra-2

Figure 4